



Minerva Access is the Institutional Repository of The University of Melbourne

Author/s:

Schneider, E;El Hajj, N;Richter, S;Roche-Santiago, J;Nanda, I;Schempp, W;Riederer, P;Navarro, B;Bontrop, RE;Kondova, I;Scholz, CJ;Haaf, T

Title:

Widespread differences in cortex DNA methylation of the "language gene" *CNTNAP2* between humans and chimpanzees

Date:

2014-04-01

Citation:

Schneider, E., El Hajj, N., Richter, S., Roche-Santiago, J., Nanda, I., Schempp, W., Riederer, P., Navarro, B., Bontrop, R. E., Kondova, I., Scholz, C. J. & Haaf, T. (2014). Widespread differences in cortex DNA methylation of the "language gene" *CNTNAP2* between humans and chimpanzees. *EPIGENETICS*, 9 (4), pp.533-545. <https://doi.org/10.4161/epi.27689>.

Persistent Link:

<https://hdl.handle.net/11343/250428>

License:

CC BY-NC

Widespread differences in cortex DNA methylation of the “language gene” *CNTNAP2* between humans and chimpanzees

Eberhard Schneider¹, Nady El Hajj¹, Steven Richter¹, Justin Roche-Santiago¹, Indrajit Nanda¹, Werner Schempp², Peter Riederer³, Bianca Navarro⁴, Ronald E Bontrop⁵, Ivanela Kondova⁵, Claus Jürgen Scholz⁶, and Thomas Haaf^{1,*}

¹Institute for Human Genetics; Julius Maximilian University; Würzburg, Germany; ²Institute for Human Genetics; University of Freiburg; Freiburg, Germany;

³Clinical Neurochemistry Laboratory; Department of Psychiatry; University Hospital; Würzburg, Germany; ⁴Institute of Legal Medicine; University Medical Center; Mainz, Germany; ⁵Biomedical Primate Research Center; Rijswijk, The Netherlands; ⁶Laboratory for Microarray Applications; IZKF; Julius Maximilians University; Würzburg, Germany

Keywords: *CNTNAP2*, DNA methylation, human brain evolution, human-chimpanzee comparison, human-specific communication, language

Abbreviations: aa, amino acid; ASD, autism spectrum disorder; CpG, cytosine phospho(diester bond) guanine; DMR, differentially methylated region; HSA, Homo sapiens; LCB, local collinear block; MAD, median absolute deviation; MAF, minor allele frequency; MeDIP, methylated DNA immunoprecipitation; PTR, Pan troglodytes; QUASEP, quantification of allele-specific expression by pyrosequencing; qPCR, quantitative real-time polymerase chain reaction; RMS, relative methylation score; rRMS, region-specific RMS; SLR, signal log₂ ratio; SNP, single nucleotide polymorphism

CNTNAP2, one of the largest genes in the human genome, has been linked to human-specific language abilities and neurodevelopmental disorders. Our hypothesis is that epigenetic rather than genetic changes have accelerated the evolution of the human brain. To compare the cortex DNA methylation patterns of human and chimpanzee *CNTNAP2* at ultra-high resolution, we combined methylated DNA immunoprecipitation (MeDIP) with NimbleGen tiling arrays for the orthologous gene and flanking sequences. Approximately 1.59 Mb of the 2.51 Mb target region could be aligned and analyzed with a customized algorithm in both species. More than one fifth (0.34 Mb) of the analyzed sequence throughout the entire gene displayed significant methylation differences between six human and five chimpanzee cortices. One of the most striking interspecies differences with 28% methylation in human and 59% in chimpanzee cortex (by bisulfite pyrosequencing) lies in a region 300 bp upstream of human SNP rs7794745 which has been associated with autism and parent-of-origin effects. Quantitative real-time RT PCR revealed that the protein-coding splice variant *CNTNAP2*-201 is 1.6-fold upregulated in human cortex, compared with the chimpanzee. Transcripts *CNTNAP2*-001, -002, and -003 did not show skewed allelic expression, which argues against *CNTNAP2* imprinting, at least in adult human brain. Collectively, our results suggest widespread cortex DNA methylation changes in *CNTNAP2* since the human-chimpanzee split, supporting a role for *CNTNAP2* fine-regulation in human-specific language and communication traits.

Introduction

In the evolutionary history of primates the two most distinctive traits that have been attributed exclusively to humans are language and enlarged brain size. Language may be both a driving force as well as an outcome of accelerated brain evolution.¹ In order to better understand the mechanisms underlying the co-evolution of language and brain size, it is helpful to elucidate the biological and molecular basis of language. Considering the ease of language acquisition in children, language must have some inherited components which should be reflected in the human genome and/or epigenome.^{2,3} There are at least two key features, “recursion” and “theory of mind,” which are thought to be

essential for the human-specific faculty of language. Recursion is the generation of an infinite range of expressions from a finite set of elements,² whereas the theory of mind enables an individual to assess the mental state of other individuals.⁴ In particular the latter is severely impaired in individuals with autism spectrum disorders (ASD).⁵ In this light, it is tempting to speculate that ASD genes have been important for the development of human-specific communication and/or language traits.

When looking for genetic factors that may have played a role in the evolution of the theory of mind, one of the most prominent candidates is the contactin associated protein-like 2 (*CNTNAP2*) gene. It encodes a neurexin which is essential for development of the vertebrate central nervous system and is highly expressed

*Correspondence to: Thomas Haaf; Email: thomas.haaf@uni-wuerzburg.de

Submitted: 09/25/2013; Revised: 12/06/2013; Accepted: 12/30/2013; Published Online: 01/16/2014
<http://dx.doi.org/10.4161/epi.27689>

in the developing human cortex. It functions as a cell adhesion protein and receptor mediating interaction between neurons and glia cells.^{6,7} Heterozygous sequence variants/mutations in *CNTNAP2* have been associated (sometimes with small effect size) with language impairment⁸⁻¹² and a broad range of neurodevelopmental phenotypes including ASD,¹³⁻¹⁶ attention deficit hyperactivity disorder, epilepsy, schizophrenia, and Gilles de la Tourette syndrome.¹⁷⁻¹⁹ Homozygous or compound heterozygous mutations cause severe epilepsy, mental retardation, and Pitt-Hopkins syndrome.^{20,21} *CNTNAP2* is physically and functionally linked to the forkhead box P2 (*FOXP2*) gene, which also has been implicated in speech and language development.^{22,23} *FOXP2* and *CNTNAP2* are located on human chromosome 7q31 and 7q35, respectively, in a chromosome segment that is highly enriched with communication-associated genes.²⁴ The transcription factor *FOXP2* directly binds to the *CNTNAP2* gene and downregulates it.⁸ Both *FOXP2* and *CNTNAP2* have been targets of Darwinian selection during recent human evolution.^{25,26}

The genetic differences between humans and our closest relatives, the chimpanzees consist of approximately 1% fixed single-nucleotide substitutions and 3% euchromatic divergence due to insertion and deletion events.^{27,28} In this light, it is plausible to assume that the human-specific communication and language phenotypes are mainly due to changes in gene regulation rather than structural changes in the gene products. Indeed, comparative transcriptome analyses revealed substantial expression differences between human and chimpanzee tissues, in particular in the brain.²⁹⁻³⁵ A subset of genes showed elevated expression in the human brain after the split from the chimpanzee lineage.²⁹⁻³¹ Epigenetic mechanisms, which control the temporal, spatial, and parent-specific gene expression patterns, may underlie a considerable part of these gene expression differences between humans and chimpanzees. Epigenetic information is not encoded by the DNA sequence itself but by reversible modifications of DNA and/or histones, that can be transmitted from cells to daughter cells. Promoter DNA methylation during development or disease processes is associated with posttranslational histone modifications that lead to a locally condensed inactive chromatin structure and gene silencing.^{36,37}

Genome-wide comparisons in different human and chimpanzee tissues revealed that although overall the tissue-specific DNA methylation patterns are conserved between species a subset of gene promoters and other sequences (i.e., certain retrotransposon subfamilies) exhibit striking methylation differences.³⁸⁻⁴¹ Candidate gene analyses also showed differential DNA methylation and expression between human and non-human primate brains,^{42,43} supporting a role for human-specific DNA methylation in brain evolution. The observation that intragenic DNA methylation is more frequent than at promoters suggests biological functions of DNA methylation in addition to gene silencing by blocking the binding of transcriptional activators to the promoter region. Gene body methylation may play a role in exon definition, i.e., by a higher methylation than in the flanking introns, modulating alternative RNA splicing.⁴⁴⁻⁴⁸

CNTNAP2 is a prime candidate gene for the theory of mind phenotype in the human faculty of language and, therefore, a probable target for epigenetic evolutionary changes. In this study we compared the cortex methylation patterns of the human and chimpanzee orthologs using custom-designed ultra-high resolution NimbleGen tiling arrays for both the human and the chimpanzee *CNTNAP2* and identified differentially methylated regions (DMRs) throughout the entire gene. A minor protein-coding splice variant of *CNTNAP2* is significantly upregulated in human cortex.

Results

High-resolution analysis of human and chimpanzee *CNTNAP2* methylation patterns

Figure 1 presents an overview of the *CNTNAP2* methylation analysis in human and chimpanzee cortices. Custom-designed human and chimpanzee 12x35K NimbleGen tiling arrays were used to compare the cortex methylation patterns of human and chimpanzee *CNTNAP2* at ultra-high resolution. The arrays covered the entire gene (2.3 Mb) and ~200 kb flanking sequence, representing approximately 1.6% of human chromosome 7. Following enrichment of methylated DNA, MeDIP vs. input DNA of six human and five chimpanzee brain samples (Table 1) was hybridized in duplicates to the human and chimpanzee array, respectively. All samples yielded detectable signals passing the required NimbleGen quality standards. After data normalization, smoothing, and correction for CpG density, the obtained relative methylation scores (RMSs) were mapped to an optimized human-chimpanzee sequence alignment that was corrected for microrearrangements and species-specific changes. All sequences such as repeats and segmental duplications that could not be mapped unequivocally in the human and chimpanzee genome, respectively, were excluded from this alignment. Using the Mauve alignment tool,^{49,50} we defined 42 local collinear blocks (LCBs) with highly similar sequence stretches in human and chimpanzee. Of these, 19 blocks with sufficient probe coverage in both species, namely LCBs 1, 6, 8, 9, 10, 14, 15, 16, 17, 20, 25, 27, 29, 30, 32, 33, 38, 40, and 42 were considered for further analysis (Fig. S1).

In order to analyze the signals on the array, we developed a customized algorithm for appropriate qualification and quantification of the data. Because comparison of single CpG sites between species is overstraining the accuracy of an array-based approach, we defined 3461 regions in the 19 LCBs based on the microarray signals. Regions with less than one CpG in each species were excluded from further analysis, resulting in 2623 regions, which could be compared between humans and chimpanzees. The median size of the latter regions was 463 bp (MAD 368 bp, range 4115 bp, min 100 bp, max 4215 bp). Details (genomic coordinates, median MeDIP signals, human-chimpanzee signal differences, etc.) are presented in Table S1. The 3461 originally defined regions covered 1.76 Mb (70.1%) and the 2623 further analyzed regions 1.59 Mb (63.4%) of the entire human array (2.51 Mb). Of the 2623 analyzed regions containing one or usually more than one CpG in both species,

1753 (66.8%) were equally methylated in human and chimpanzee brain; 870 (33.2%) displayed region-specific (cumulated) RMSs (rRMSs) with Benjamini-Hochberg adjusted false discovery rates between 0.017 and 0.046, indicating significant MeDIP signal differences between the two species. Altogether, 420 DMRs showed a higher and 450 a lower methylation signal in human than in the chimpanzee brain. For each of the 2623 regions containing CpGs in each species, the rRMSs of six human and five chimpanzee cortices displayed fairly similar variances in both species. DMRs tended to have a slightly lower common (human and chimpanzee) variance than equally methylated regions (Fig. S2).

Figure 2A presents the rRMSs of the 870 DMRs along the *CNTNAP2* region. Altogether, these DMRs amount to 0.34 Mb (21%) of the analyzed 1.59 Mb sequence. The diagrams at the bottom (Fig. 2B–E) zoom into four smaller DNA segments containing the differentially methylated regions B (in intron 2), C (in exon 17), E, and F (in intron 20). These DMRs are distinguished from neighboring equally methylated regions by standard deviations that do not overlap between the calculated human rRMSs (six samples) and chimpanzee rRMSs (five samples). Table 2 shows the distribution of DMRs in the genomic context of the analyzed region. The highest density of DMRs is found in exons and the lowest in the promoter region. Compared with introns, exons are approximately 2.5-fold enriched with DMRs. Interestingly, DMRs are found at the exon-intron boundaries of human exon 3 (start and end), human and chimpanzee exon 7 (start), human and chimpanzee exon 10 (end), and human and chimpanzee exon 23 (start and end).

In order to identify linear variables that account for most of the variance, a correspondence analysis of the entire data set was performed. This analysis revealed two main components which together explain approximately 60% of the variance. Plotting the analyzed individuals on the two main components (Fig. 3) revealed a clear separation between humans and chimpanzees on the horizontal axis (accounting for 41.4% of the observed variance) and a tentative separation between males and females on the vertical axis (accounting for 18.2% of the variance).

Bisulfite pyrosequencing

To validate the array results, we quantified the methylation of seven regions (Fig. 4) by bisulfite pyrosequencing in 11 human and 6 chimpanzee brain samples (Table 1); region A in the pyrosequencing analysis corresponds to region 83 of LCB8 in the microarray experiment (Fig. 2), B to 64/LCB17, C to 391/LCB38, D to 395/LCB38, E to 520/LCB38, F to 542/LCB38, and G to 17/LCB40 (Tables S1 and S2). According to the microarray experiment, region C had significantly increased, whereas regions B, E, and F had significantly decreased DNA

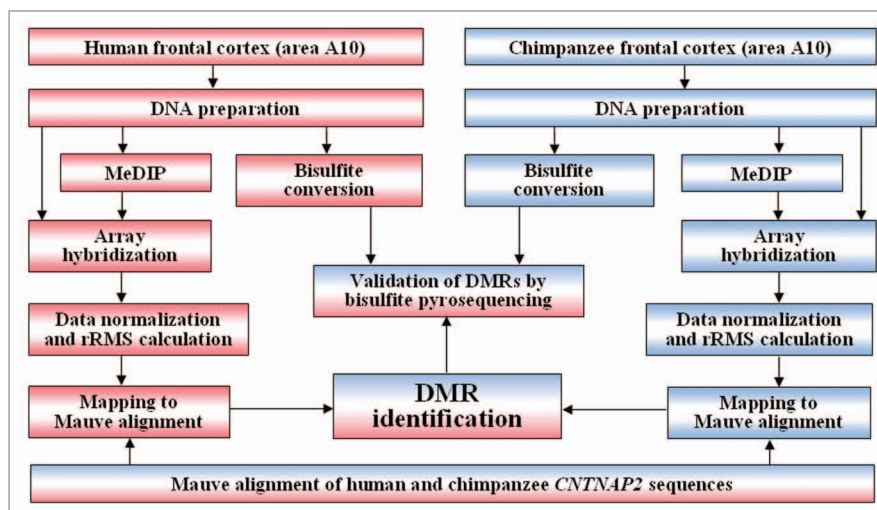


Figure 1. Flowchart of comparative *CNTNAP2* methylation analysis in human and chimpanzee cortices. Methylated DNA immunoprecipitation (MeDIP) with NimbleGen tiling arrays was used to identify methylation differences between human and chimpanzee cortex *CNTNAP2* at ultra-high resolution. Region-specific relative methylation scores (rRMSs) from both species were mapped to an optimized human-chimpanzee MAUVE sequence alignment. A few differentially methylated regions (DMRs) were validated by bisulfite pyrosequencing in human and chimpanzee cortex DNA.

methylation in the human brain, compared with the chimpanzee (Table 3). The pyrosequencing assays were located within or in close proximity (<1 kb distance) to the regions targeted by the microarray. All four DMRs in the microarray experiment also displayed significant (Mann-Whitney U test) between-species differences in the same direction by bisulfite pyrosequencing (Table 3). Regions A, D, and G did not show significant brain methylation differences between humans and chimpanzees in both microarray and pyrosequencing analyses.

The most pronounced difference ($P < 0.001$) with 28% median methylation in human and 59% in chimpanzee brains was observed by bisulfite pyrosequencing in region B (human chr.7: 146488940 to 146489309 bp; Ensembl version 59), in close proximity to human single nucleotide polymorphism (SNP) rs7794745 (chr.7: 146489606 bp) which has been associated with ASD and parent-of-origin effects.¹⁴ Region B lies in intron 2 of the main transcript *CNTNAP2*-001. It contains four CpGs in humans and five in chimpanzees, three of which are conserved between species. Pyrosequencing of six human and six chimpanzee blood DNAs revealed hypermethylation of region B in both humans (median 91%, range 90–92%) and chimpanzees (median 93%, range 92–94%), with a slightly higher methylation in the chimpanzee. Although the between-species methylation difference was much less pronounced in white blood cells than in cortex, it was also significant (Mann-Whitney U test, $P = 0.009$) and in the same direction.

Expression of human and chimpanzee *CNTNAP2* transcripts

Both human and chimpanzee *CNTNAP2* have different transcripts which are expressed in the brain (Figs. 2 and 4). The full-length (9894 bp) transcript *CNTNAP2*-001 has 24 exons

Table 1. Cortex samples

Individuals	Sex	Age	Age class	NimbleGen array	Bisulfite pyroseq.	qPCR	QUASEP
Humans							
HSA1	f	24	early adult		•		•
HSA2	m	40	late adult		•	•	
HSA3	m	54	late mature	•	•		•
HSA4	m	31	late adult	•	•		
HSA5	m	39	late adult	•	•		•
HSA6	m	44	early mature	•	•		
HSA7	f	83	senile	•	•		
HSA8	m	41	early mature	•	•		
HSA9	m	40	late adult		•		
HSA10	m	45	early mature		•		•
HSA11	m	73	senile		•		
HSA13	m	51	late mature			•	
HSA15	f	33	late adult			•	
HSA16	m	64	senile			•	
HSA18	f	54	late mature			•	
HSA20	f	79	senile			•	
HSA22	m	48	early mature			•	
HSA23	m	35	late adult			•	
HSA24	m	51	late mature			•	
HSA25	m	45	early mature			•	
Chimpanzees							
PTR1	m	14	late adolescence	•	•	•	
PTR2	m	7	early adolescence	•	•	•	
PTR3	f	40	old age (senile)	•	•	•	
PTR4	f	12	early adolescence	•	•		
PTR5	f	42	old age (senile)	•	•	•	
PTR6	f	43	old age (senile)		•	•	

encoding a 1,331 amino acid (aa) protein. The minor splice variant *CNTNAP2*-201 (1944 bp) has nine exons, of which seven are coding for a 390 aa protein. *CNTNAP2*-002 (556 bp) has four exons encoding a 185 aa protein. *CNTNAP2*-003 consists of four non-coding exons. We designed intron-spanning quantitative real-time RT PCR (qPCR) assays (Fig. 4) to compare the expression of transcripts *CNTNAP2*-001, -201, and 003 in human and chimpanzee cortices. Following validation of candidate reference genes,^{51,52} *SDHA* and *EIF2B2* were used for normalization of the *CNTNAP2* mRNA expression levels in human and chimpanzee brain. *CNTNAP2* transcript levels were measured by qPCR in ten human and five chimpanzee cortices (Table 1). Data analysis with the delta-delta c(t) method⁵³ revealed a slightly higher expression of all three measured transcripts in the human compared with the chimpanzee brain (Fig. 5); the 1.6-fold upregulation of transcript *CNTNAP2*-201 in humans was significant ($P = 0.02$). In humans (seven male vs. three female samples), none of the transcripts was differentially

expressed between sexes. In the chimpanzee brain, the full-length transcript *CNTNAP2*-001 showed 1.4-fold higher expression in female brain, however because of the low number of analyzed samples (three males vs. two females) this result should be considered as preliminary.

Because *CNTNAP2* was reported to exhibit parent-specific effects,^{12,14} we wanted to study allele-specific expression of *CNTNAP2* transcripts in human cortex tissue. To this end, we typed three transcribed SNPs in human brain samples and identified four heterozygous individuals for Quantification of Allele-specific Expression by Pyrosequencing (QUASEP).⁵⁴ SNP rs10240503 (present in *CNTNAP2*-001 and -002) showed an allelic ratio of 0.51/0.49 in human brain HSA10, rs2530310 (*CNTNAP2*-002 and -003) a ratio of 0.50/0.50 in HSA5, and rs2717820 (*CNTNAP2*-001 and -003) a ratio of 0.45/0.55, 0.47/0.53, and 0.49/0.51, respectively, in HSA1, 3, and 5. Collectively, these results strongly argue against preferential expression of one parental allele (at least for the tested isoforms)

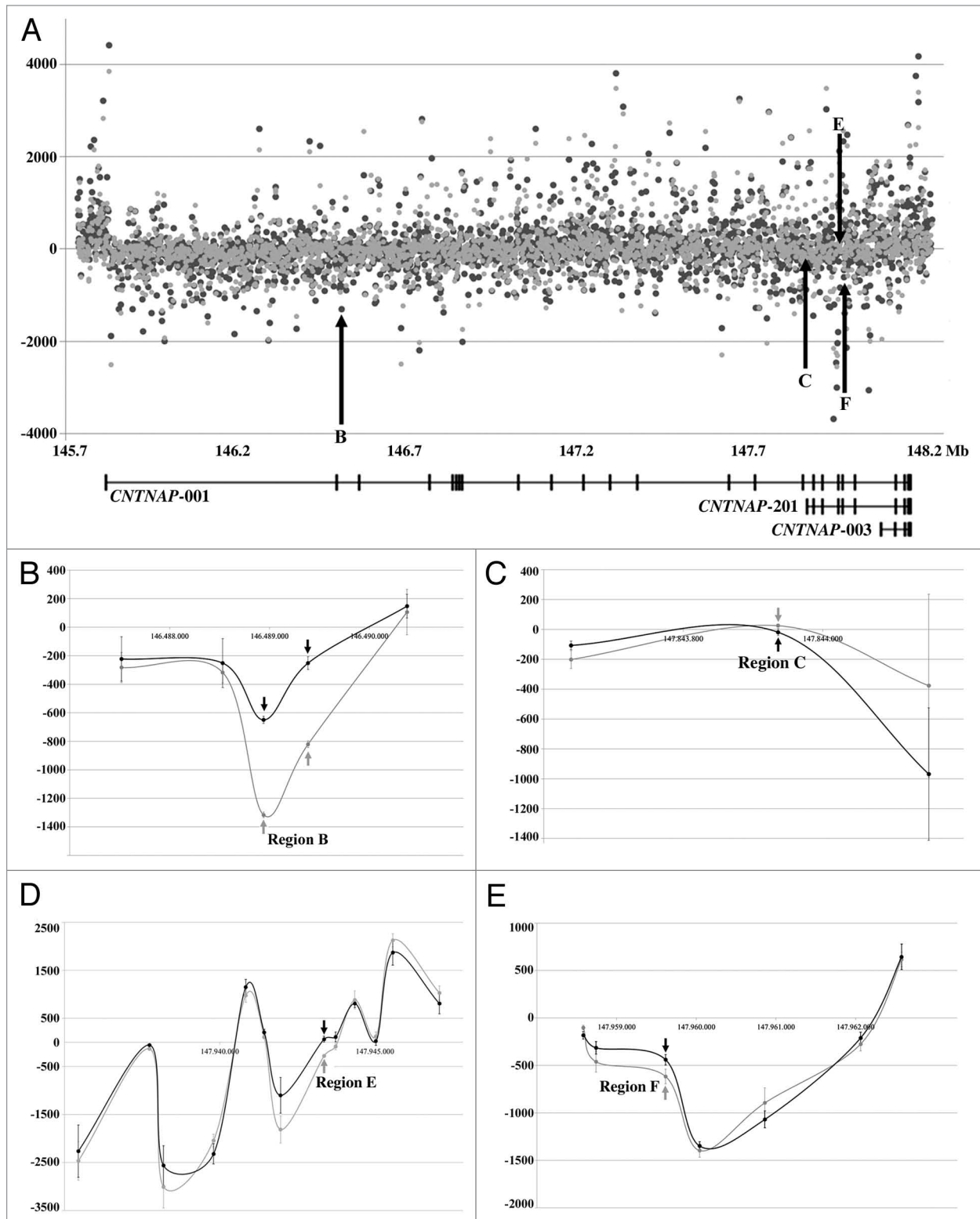


Figure 2. Methylation comparison of human and chimpanzee *CNTNAP2* gene and flanking sequences using NimbleGen tiling array. The vertical axis represents the relative methylation scores (rRMSs), the horizontal axis the locations of the analyzed regions along the 2.51 Mb human reference sequence. For better orientation, the exon-intron structure of transcripts *CNTNAP2*-001, -201, and -003 is shown below the abscissa. Gray dots indicate human and black dots the orthologous chimpanzee regions. **(A)** Diagram showing the distribution of the 870 regions with significant between-species methylation differences in the analyzed *CNTNAP2* region, altogether representing 0.34 Mb of the 2.51 Mb reference sequence. Vertical arrows indicate four DMRs (regions B, C, E, and F), which were validated by bisulfite pyrosequencing (Table 3). **(B–E)** Zooms into four smaller DNA segments (indicated by arrows in **A**) showing both equally and differentially methylated regions. DMRs are indicated by gray (human rRMSs) and black (chimpanzee rRMSs) arrows. Bars represent the standard deviation of the six measured human and the five chimpanzee samples, respectively.

Table 2. Distribution of CpGs and DMRs in the *CNTNAP2* region

	Human					Chimpanzee				
	Length (bp)	Number of CpGs	Relative CpG density ^a	Number of DMRs ^b	Relative DMR enrichment ^c	Length (bp)	Number of CpGs	Relative CpG density ^a	Number of DMRs ^b	Relative DMR enrichment ^c
Upstream ^d	95 000	725	1.00	54	4.26	95 000	676	1.00	54	4.26
Promoter ^e	7 500	145	2.53	1	1.00	7 500	146	2.74	1	1.00
Exons	9 894	199	2.64	8	6.06	9 910	194	2.75	8	6.05
Introns	2 294 744	17 695	1.01	757	2.47	2 336 584	18 032	1.08	757	2.43
Downstream ^f	99 996	1 340	1.76	54	4.05	99 996	1 266	1.78	54	4.05

^aNumber of CpGs divided by number of nucleotides, scaled to the minimum (= 1) within each species. ^bThe number of DMRs (874) in this table is slightly higher than 870, because a few DMRs can be classified into different genomic contexts, i.e., promoter and first exon. ^cDMR counts divided by the number of nucleotides, scaled to the smallest value (= 1). ^dSequence located >5000 bp upstream of the first exon base. ^eSequence from 5000 bp upstream to 2499 bp downstream the first exon base. ^fSequence downstream of the last exon base.

and genomic imprinting. Unfortunately, none of the chimpanzee samples was informative for one of these SNPs.

Discussion

Although humans usually claim a unique position among the clade of primates, there may be no sharp boundary but a more or less gradient transition between human and non-human primates.⁵⁵ Enhanced communication abilities, in particular the faculty of language are arguably the most distinctive trait attributed to humans. It is plausible to assume that human-specific cognitive abilities have their structural basis in the enlarged human brain. Fossil records indicate that absolute cranial capacity started to increase about 2–3 million years ago.⁵⁶ Because it is not possible to analyze the genome or to reconstruct the communication abilities of *Homo habilis* who first showed an enhanced encephalization quotient, inferential methods, i.e., comparisons between human and chimpanzee brains are used to identify the genetic and epigenetic basis of human language evolution. Considering that the genetic differences between humans and chimpanzees are rather small,^{27,28} the human-specific cognitive and communication abilities are more likely due to changes in gene regulation rather than to structural changes in the gene products.

Methylation differences between human and chimpanzee cortices

Numerous studies have linked *CNTNAP2* to human language abilities,^{8,10,12} autism,^{13–16} and other neurodevelopmental disorders with impaired communication.^{9,11,19} The main goal of this study was to identify epigenetic signatures supporting a role for *CNTNAP2* in the co-evolution of the human brain and language. To this end, we compared the human and chimpanzee cortex methylation patterns of the entire *CNTNAP2* gene and its flanking sequences. Following alignment of the orthologous reference sequences, data normalization, smoothing, and correction for CpG content, approximately 1.59 Mb of the 2.51 Mb target region could be compared in human and chimpanzee, of which 0.34 Mb (21%) displayed significant between-species methylation differences. Because of the elevated mutability of cytosines at CpG sites,⁵⁷ the number of CpG sites in a particular

region may vary within and between species, which adds to the signal variance (Fig. S2). However, this has only a very slight effect on the CpG-density weighted signal difference between species and does not explain the high number of DMRs.

The CpG density in *CNTNAP2* exons is significantly ($P < 0.001$ in both species) higher than in introns (Table 2; Fig. S3), which may help the splicing machinery to recognize the exons and increase splicing signal strength.^{44–46} DNA methylation can affect the binding of CTCF and other splicing regulatory proteins that are recruited by methyl-binding proteins and, thus, take part in exon recognition.^{47,48} Considering the huge size of intronic sequences in the *CNTNAP2* gene, it is not surprising that the vast majority (757 of 870, 87%) of DMRs is located in introns. However, the density of DMRs in exons is more than 2-fold higher than that in introns (Table 2). In this light, it is tempting to speculate that the observed methylation differences between humans and chimpanzees modulate the exon selection process and alternative splicing. The promoter regions are not enriched with DMRs, indicating that the evolutionary forces driving epigenetic changes have acted on the entire gene and were not targeted to the promoter.

It is difficult to compare our ultra-high resolution methylation scan of a 2.51 Mb region with lower-resolution genome-wide analyses (focusing on promoter regions), which did not find differential *CNTNAP2* methylation between the human and the rhesus macaque⁴⁰ or chimpanzee brain,⁴¹ respectively. Our results show unexpectedly high between-species cortex methylation differences across the entire gene. It is conceivable that these widespread epigenetic changes affect the fine-tuning of cortex *CNTNAP2* regulation. However, the formal proof that cortex *CNTNAP2* methylation is different from genomic expectation requires ultra-high resolution control data sets which so far are missing. Our limited data on a 2.51 Mb region suggests that DMRs are not evenly distributed throughout genomic sequence. DMRs appeared to be enriched in exons, compared with introns and the promoter region. In addition, DMR density was slightly higher in the upstream than in the downstream flanking sequence. Since we do not have methylation data for an outgroup, it is also unclear which changes have occurred in the human and the chimpanzee lineage, respectively.

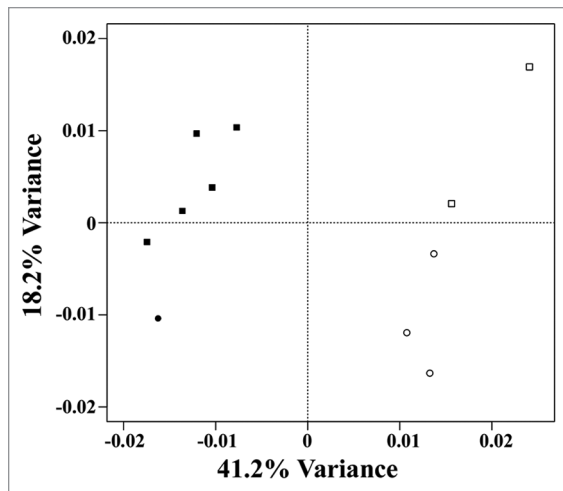


Figure 3. Correspondence analysis of the NimbleGen array data. The first axis explaining 41.4% of variance in the data set separates human (black symbols) and chimpanzee brain samples (open symbols). The second axis accounting for 18.2% of the observed variance separates males (squares) and females (circles).

Correspondence analysis clearly separated the 2 analyzed species on the first axis, explaining 41.4% of the variance in the array data set. Our experimental design using two different arrays for the analysis of human and chimpanzee methylation patterns cannot distinguish between species and array effects. Although we cannot exclude that the different array designs contribute to the observed variance, it is very unlikely that the high variance on the first axis is caused by the platform effect alone. Microarray data provide relative methylation scores, which allow one to pinpoint regions with higher and lower DNA methylation in the one or other species, whereas bisulfite pyrosequencing quantifies the absolute methylation levels of selected regions with high accuracy (in the order of several percentage points). It is reassuring that several regions (tentatively called A-G) that were or were not predicted to exhibit between-species methylation differences by microarrays could be validated by quantitative bisulfite pyrosequencing. It is worth emphasizing that the 369-bp region B, which is significantly ($P < 0.001$) hypomethylated in humans (28%) compared with chimpanzees (59%) lies < 300 bp downstream of SNP rs7794745 in intron 2 of the full-length transcript *CNTNAP2*-001, which has been associated with an increased risk for autism.¹⁴ In addition, region B overlaps with a DNase sensitive regulatory site (ENSR00001564819) in human embryonic stem cells (Fig. 4). Assuming lower communication (in particular theory of mind) abilities of chimpanzees compared with humans, it is tempting to speculate that aberrant methylation of such species-specifically methylated regions contributes to the communication and language impairment in ASD. One plausible approach toward identification of (epi)genetic changes underlying human neurodevelopmental disorders is defining the molecular changes during the evolution of human-specific (e.g., language, disease susceptibility) phenotypes.⁵⁸ Although region B was hypermethylated in both human and chimpanzee blood, there was a small but significant between-species methylation

difference in the same direction. Assuming that despite enormous between-tissue differences the blood epigenome can reflect at least to some extent the methylation variation in the brain,^{59,60} *CNTNAP2*-region B blood DNA methylation may be exploited as an epigenetic biomarker for human neurodevelopmental disorders.

Parent-of-origin and sex effects

Considering sex-specific effects in language processing,^{61,62} it is not unexpected that the second axis of the correspondence analysis separated males and females, gender-specific *CNTNAP2* methylation differences explaining 18.2% of the variance in the data set. However, since only one female vs. five male human brain samples was hybridized to the human array, this sex-specific effect should be considered with caution. The separation between three female and two male brain samples on the chimpanzee array appears to be more robust. Follow-up experiments with a larger number of samples are needed to prove sex-specific *CNTNAP2* methylation.

Differential parent-of-origin expression of *FOXP2*⁶³ and its target *CNTNAP2*¹⁴ have been suggested to play a role in speech development. Recently, it was shown that *CNTNAP2* variants (rs2710102 and rs7794745) that are associated with language impairment and ASD have functional effects on brain activation in healthy individuals during a language processing task.¹² Activation of the right (contralateral) Broca area homolog was more pronounced in individuals with putative risk alleles, in particular when the T allele of rs7794745 was inherited from mother to son. One obvious explanation for preferential or exclusive expression of one of the two parental alleles, i.e., in the brain, is genomic imprinting. The parent-specific epigenetic marks of imprinted genes are established in the male or female germline, respectively, and then maintained after fertilization and during further development.^{64,65} Imprinted genes are not only essential for the regulation of fetal and placental growth and somatic differentiation,⁶⁶ but also for brain development, neurological, and behavioral functions.⁶⁷ It has been hypothesized that genomic imprinting has played a major role in the evolution of the social human brain^{68,69} and language.⁷⁰

The parental conflict hypothesis⁷¹ postulates that genomic imprinting in mammals evolved because of conflicting maternal and paternal interests in the allocation of maternal resources to the offspring with paternally expressed genes enhancing and maternally expressed genes limiting fetoplacental growth. The parental antagonism theory of language evolution⁷⁰ extends this hypothesis. The higher than expected frequency of involvement of X-chromosomal and imprinted genes in language phenotypes and the greater divergence of maternally than paternally expressed genes between humans and chimpanzees are consistent with the view that language emerged during an evolutionary struggle between parental genomes with the human-specific and cooperative aspects of language reflecting the maternal interests.⁷⁰ However, allelic expression analysis of transcripts *CNTNAP2*-001, -002, and -003 did not provide any evidence for *CNTNAP2* imprinting in adult human brain. Previously, it has been shown that *FOXP2* also lacks parent-specific expression in human brain.⁷²

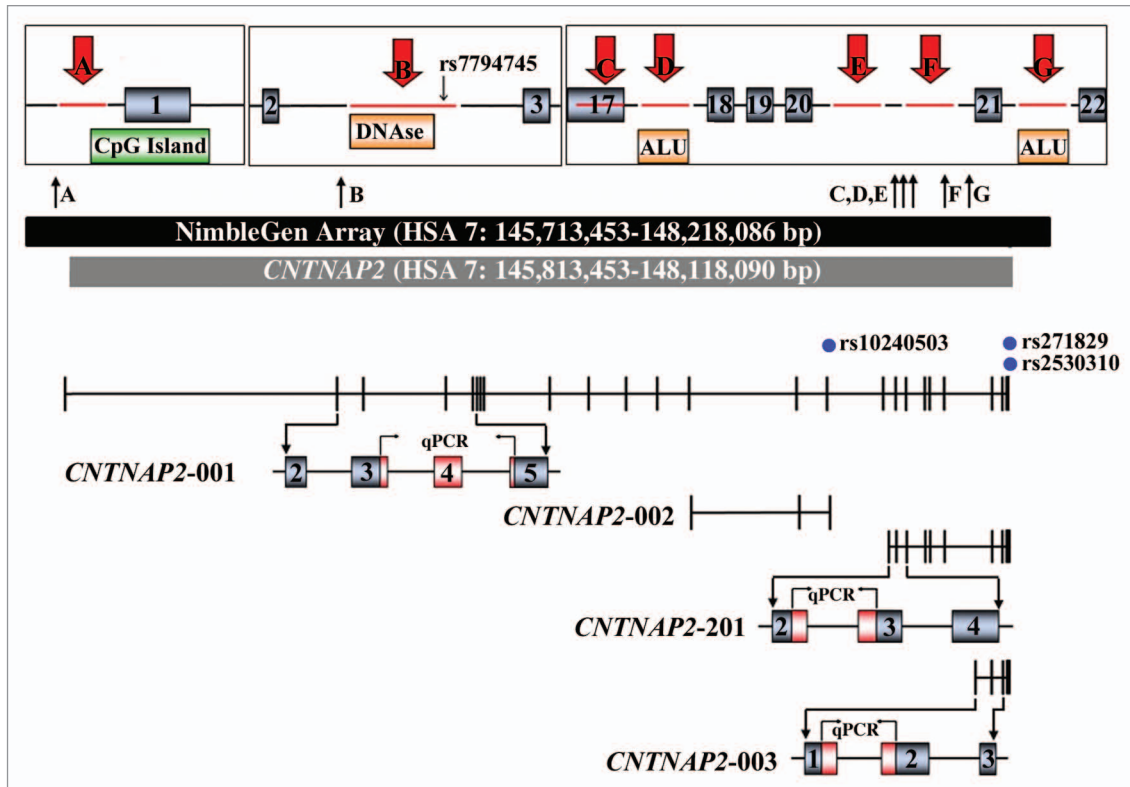


Figure 4. Physical map of the analyzed region. The black bar indicates the region on human chromosome 7q35 covered by the array, the gray bar the *CNTNAP2* gene sequence. The upper part zooms in specific regions of the gene, indicating the location of exons and regulatory sites. Vertical thin black and thick red arrows highlight the DNA segments (red lines) that have been analyzed by bisulfite pyrosequencing assays A–G. The bottom part of the figure shows the exon-intron structure of different *CNTNAP2* transcripts. The red shaded exon sequences were amplified by transcript-specific qPCR. Blue dots indicate the location of SNPs for QUASEP.

Expression differences between human and chimpanzee cortices

Consistent with our study, several microarray-based transcriptome analyses provided evidence for differential *CNTNAP2* expression in human and chimpanzee cortices.^{32,33,43} In contrast, RNA sequencing did not detect human-specific upregulation in the cerebellum.^{34,35} Our isoform-specific qPCR results suggest that the increased *CNTNAP2* mRNA levels in human cortex are mainly due to significant (1.6-fold) upregulation of the protein-coding minor transcript *CNTNAP2-201*. The full-length transcript *CNTNAP2-001* and the non-coding transcript *CNTNAP2-003* showed comparable expression levels in human and chimpanzee cortices. Although intuitively differential *CNTNAP2* methylation and expression are assumed to be linked, at present they must be considered as independent findings. Differential human-chimpanzee methylation was observed across the entire gene, whereas differential expression was detected for only one of three studied isoforms. This may be partially due to the limited power of qPCR expression analysis, compared with our ultra-high resolution methylation scan. In this light, it will be interesting to correlate the observed widespread brain *CNTNAP2* methylation differences with future higher-resolution RNA sequencing data sets.

Caveats and conclusions

Our study provides a comprehensive cortex methylation analysis of *CNTNAP2*, one of the largest and arguably most interesting genes in human brain evolution and function. One important caveat of comparative studies in human and chimpanzee brains is the low sample size, which makes it difficult to reach statistical significance and to exclude confounding factors (such as sex, age, cause of death, and postmortem time). Moreover, all experiments were performed with frozen brain tissues, of which it was not possible to isolate specific cell types in high enough numbers. Although the cortex area A10 has a similar overall tissue architecture in human and chimpanzee brains,⁷³ differences in cell type compositions affecting the overall methylation/expression levels cannot entirely be excluded. Nevertheless, our results are consistent with the view that widespread differences in the epigenetic modification of the *CNTNAP2* gene occurred since the human-chimpanzee split 5–8 million years ago.^{74,75} The evolutionary dynamics of *CNTNAP2* methylation and expression taken together with the manifold associations of *CNTNAP2* with human reading/language abilities and a broad spectrum of neurodevelopmental disorders^{9,11,16,19} promote the idea that fine-tuning of brain *CNTNAP2* regulation has been important for the evolution of human-specific language and communication traits. Accumulating experimental evidence suggests that genetic and

Table 3. Comparison of methylation levels of selected regions between human and chimpanzee cortices

		NimbleGen arrays							
		Analyzed regions							
		A	B	C	D	E	F	G	
Human	Number of individuals	6	6	6	6	6	6	6	
	Relative methylation score	403	-1316	24	-1	-283	-617	-946	
	Standard deviation	599	146	9	103	22	77	187	
Chimpanzee	Number of individuals	5	5	5	5	5	5	5	
	Relative methylation score	-220	-650	-19	-135	66	-440	-463	
	Standard deviation	240	75	23	148	63	55	232	
		<i>P</i> value ^a	0.350	0.017	0.017	0.210	0.017	0.027	0.106
		Bisulfite pyrosequencing							
		Analyzed regions							
		A	B	C	D	E	F	G	
Human	Number of individuals	7	9	5	6	7	7	11	
	Median methylation (%)	79	28	94	97	84	16	96	
	Standard deviation	4	6	1	1	3	2	2	
Chimpanzee	Number of individuals	4	6	4	4	4	4	6	
	Median methylation (%)	84	59	90	97	93	25	94	
	Standard deviation	4	12	5	1	2	3	4	
		<i>P</i> value ^a	0.230	<0.001	0.016	0.067	0.006	0.006	0.301

^aFor between-species methylation difference.

epigenetic variation in this gene contributes to both interspecific and interindividual differences in brain development and function.

Materials and Methods

This study was approved by the ethics committee of the Landesärztekammer Rheinland-Pfalz and samples exploited with full consent of the BrainNET Europe Consortium (<http://www.brainnet-europe.org>).

Brain samples (Table 1) were obtained between 2 and 7 h postmortem from six chimpanzees (*Pan troglodytes*, PTR) and within one day from 25 humans (*Homo sapiens*, HSA). Age classes of human and chimpanzees were determined according to Knussmann⁷⁶ and Godall,⁷⁷ respectively. Frontal cortex tissue area A10 was dissected from the frontal pole and immediately frozen at -80 °C until further use. Genomic DNA and RNA were extracted using the Precellys Tissue DNA and RNA kit, respectively (PEQLAB). Different subsets of cortex samples were used for array hybridization, bisulfite pyrosequencing, qPCR, and QUASEP (Table 1). Amount and quality of the brain DNA and RNA samples, respectively, were determined with a Nanodrop spectrophotometer (NanoDrop Inc.). The ratio of absorbances at 260 nm vs. 280 nm was around 1.8 for DNA and around 2.0 for RNA samples. In addition, genomic DNA was extracted from 6 human and 6 chimpanzee whole blood samples using a standard salt extraction method.

NimbleGen methylation array design and MeDIP

Two different 12x135K NimbleGen DNA methylation arrays for the human and chimpanzee *CNTNAP2* gene plus 100 kb upstream and 100 kb downstream flanking sequence were designed by the Roche NimbleGen bioinformatics group. Probe design was based on reference sequences from the UCSC genome browser (<http://genome.ucsc.edu>) human build hg19 (chr.7: 145713453–148218086 bp) and chimpanzee build panTro2 (chr.7: 146592820–149139309 bp). Near-isothermal probes varying from 50 to 75 nucleotides in length were spotted on the array with a 13 bp-spacing on average. Repetitive DNA elements representing approximately 17% of the human and 20% of the chimpanzee target DNA were excluded.

Immunoprecipitation of methylated DNA was performed using the MagMeDIP kit (Diagenode) according to the manufacturer's protocol. Before MeDIP the genomic DNA was sheared with a Diagenode bioruptor to fragment sizes from 100 bp to 600 bp. Approximately 1.5 µg of sheared DNA was incubated with monoclonal anti-5-methylcytosine antibodies, bound to magnetic beads at 4 °C overnight and purified with DNA isolation buffer. qPCR with primers for *GAPDH* and *TSH2B* (Diagenode) was used to estimate the amount of enrichment of methylated DNA in the MeDIP samples vs. untreated input DNA. qPCR was performed with the RotorGene Q real-time PCR system (Qiagen). The reaction mixture contained 1x SYBR green master mix (Roche Diagnostics) and 10 µM each of forward and reverse primer in a volume of 25 µl. PCR cycling

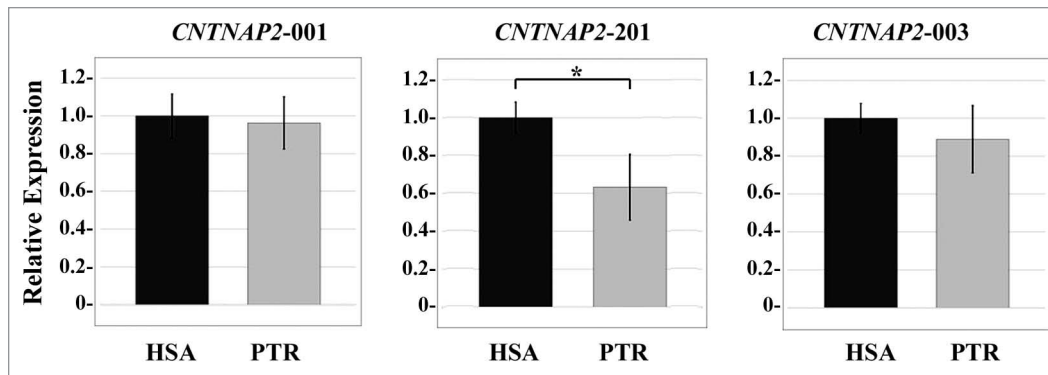


Figure 5. Relative expression of transcripts *CNTNAP2*-001, -201, and -003 in human (black bars) and chimpanzee (gray bars) brain. Black vertical lines indicate the standard deviation among ten human and five chimpanzee samples measured by qPCR. Relative expression level in human brains was set to one. Asterisks indicates a significant between-species difference for transcript -201.

consisted of 95 °C for 7 min, followed by 40 cycles at 95 °C for 15 s, and 60 °C for 60s, and a final step of 95 °C for 60 s. Melting curve analysis was performed with 60 cycles starting at 65 °C with 0.5 °C increments per cycle.

Both MeDIP and input DNA were amplified with the GenomePlex Complete Whole Genome Amplification 2 kit (Sigma-Aldrich) and purified using the QIAquick PCR Purification kit (Qiagen). One microgram of amplified DNA was denatured and labeled via primer extension with Cy dyes attached to 9-mer primers. A two color protocol (NimbleGen Roche) was used, labeling the input DNA with Cy3 and the MeDIP DNA with Cy5. The differentially labeled DNAs were co-hybridized to the customized human or chimpanzee 12x135K NimbleGen array for 16 h, washed, and then scanned on a MS200 microarray scanner (Illumina Inc.).

Human-chimpanzee methylation array data analysis

The microarray raw data for each species were within-sample loess normalized. The calculated MeDIP vs. input signal log₂ ratios (SLRs) were processed further using between-sample quantiles normalization. Then we applied a sliding window (400 bp) approach to transform the SLRs into smoothed SLRs. In order to map the normalized and smoothed SLRs on a consensus sequence they first had to be corrected for CpG density. Second, a consensus sequence between species had to be generated. Since the local CpG density has an impact on MeDIP efficiency, smoothed SLRs are not immediately comparable between species. To remove the CpG density bias from smoothed SLRs, we determined a coupling factor for each microarray probe and calculated relative methylation scores (RMSs) that are free from known immunoprecipitation biases due to variable CpG densities.⁷⁸ To generate a consensus sequence between human and chimpanzee we aligned the respective sequences with Mauve.^{49,50} After filtering for low probe coverage and gaps the remaining RMSs from both species were median scaled (i.e., $rms_i = rms_i - \text{median}[rms] / \text{IQR}[rms]$) and aligned to this consensus sequence. In case of overlapping probes at particular alignment positions, the mean-scaled RMS was assigned. This resulted in alignment-mapped microarray signals for between-species comparisons.

The comparison of alignment-mapped human and chimpanzee RMSs can lead to skewed results when comparing single CpG sites directly. Therefore we first defined genomic regions most likely exhibiting reliable methylation signals. Such a region was defined by (1) no overlap of signals along at least 100 bp, (2) >80% analyzed alignment positions, and (3) less than 50 bp of continuous gaps. For each base pair we determined the median of human and chimpanzee signals plus/minus twice their median absolute deviation. After that we summed up the RMSs to form the region-specific RMS (rRMS). In order to assign a region to be either differential methylated or not, the rRMSs between species were compared with Wilcoxon rank sum tests and subsequently Benjamini-Hochberg adjusted for false discovery rate.

Quantitative methylation data were described and analyzed with IBM SPSS, version 19.0.0, R software (<http://www.R-project.org>) and MS Excel (version 14.0.6129.5000). Data mining was performed in the Ensembl genome browser (<http://www.ensembl.org>) and NCBI databases (<http://www.ncbi.nlm.nih.gov>). Microarray data were deposited in MIAME compliant form at Gene Expression Omnibus (<http://www.ncbi.nlm.nih.gov/geo>) in entries GSE52948 (human) and GSE52949 (chimpanzee).

Bisulfite pyrosequencing

For validation of NimbleGen arrays we performed bisulfite pyrosequencing of selected *CNTNAP2* regions in 11 human and six chimpanzee DNA samples (Table 1). Assays quantifying the methylation levels of one or several evolutionarily conserved CpGs in the target region were designed with the PyroMark Assay Design 2.0 software (Qiagen). Primers and sequences to analyze are listed in Table S2. PCR amplifications were performed on a Tetrad 2 cyclor (BioRad) with an initial denaturation step at 94 °C for 3 min, 35–45 cycles of 94 °C for 30 s, primer-specific annealing temperature for 30 s, 72 °C for 60 s, and a final extension step at 72 °C for 10 min. The reaction mixture consisted of 2.5 µl 10x PCR buffer, 2.5 µl 50 mM MgCl₂, 2.5 µl 10 mM dNTP mix, 1.0 µl of each forward and reverse primer, 0.5 µl (2.5 U) Taq DNA polymerase (Roche Diagnostics), 14 µl PCR-grade water, and 100 ng template DNA. Bisulfite pyrosequencing was performed on a PyroMarkTMQ96 MD Pyrosequencing System

with the PyroMark Gold Q96 CDT Reagent Kit (Qiagen). Data analysis was done with the Pyro Q-CpG software (Qiagen).

Expression analysis

Aliquots of 500 ng total cortex RNA were reversely transcribed into cDNA using the SuperScriptIII First Stand Synthesis system (Invitrogen). Intron-spanning primers that are specific for transcripts *CNTNAP2*-001, -201, and -003 (Table S3) were designed using the cDNA sequence in Ensembl (version 61) and the Primer3 (version 0.4.0) program. For interspecific comparisons we relied on previously published reference genes with supposedly stable expression in human and chimpanzee brains.⁵¹ When testing the expression variation of *HMBS*, *EIF2B2*, and *SDHA* with geNORM,⁵² only *EIF2B2* and *SDHA* proved to be robust. To minimize batch effects, qPCRs of the three *CNTNAP2* transcripts and the two reference genes were performed together with five human and five chimpanzee samples (Table 1) on a RotorGene Q (Qiagen). The reaction mixture consisted of 10.0 μ l SsoFast EvaGreen Supermix (BioRad), 7.0 μ l PCR grade water, 1.0 μ l forward and reverse primer each, and 1.0 μ l cDNA template. Amplification was performed with initial denaturation at 98 °C for 2 min, and 40 cycles with 98 °C for 5 s and 55 °C for 20 s. A final melting step was performed from 65 °C to 95 °C with 1 °C increments every 5 s. Data analysis was done with delta-delta c(t) method.⁵³

QUASEP⁵⁴ was used to determine the allelic ratios of transcripts *CNTNAP2*-001, -002, and -003 in human frontal cortex. This method relies on transcribed SNPs to quantify the relative expression of both alleles. First we searched the Ensembl

database for SNPs: rs10240503 (minor allele frequency, MAF 0.24) is present in isoform *CNTNAP2*-001 and -002, rs2530310 (MAF 0.42) in -002 and -003, and rs2717829 (MAF 0.20) in -001 and -003. By Sanger sequencing (Table S4) we identified four informative individuals, which were heterozygous for one or more of these SNPs. QUASEP assays (Table S5) for the three SNPs were designed with the Pyrosequencing Assay Design Software (Biotage). Pyrosequencing was performed as described above.

Disclosure of Potential Conflicts of Interest

No potential conflicts of interest were disclosed.

Acknowledgments

Some of the human brain samples were obtained through the Netherlands Brain Bank (<http://www.brainbank.nl>).

Author Contributions

E.S., N.E.H, S.R., J.R.S., and I.N. performed the experiments. E.S., C.J.S., and T.H. performed the data analysis. W.S., P.R., B.N., R.E.B., and I.K. provided materials, participated in the data interpretation and revised the manuscript. E.S. and T.H. designed the study and wrote the manuscript.

Supplemental Materials

Supplemental materials may be found here: www.landesbioscience.com/journals/epigenetics/article/27689

References

1. Jerison HJ. The paleoneurology of language. *Ann NY Acad Sci* 1976; 280:370-82; PMID:1070931; <http://dx.doi.org/10.1111/j.1749-6632.1976.tb25501.x>
2. Hauser MD, Chomsky N, Fitch WT. The faculty of language: what is it, who has it, and how did it evolve? *Science* 2002; 298:1569-79; PMID:12446899; <http://dx.doi.org/10.1126/science.298.5598.1569>
3. Fitch WT. Unity and diversity in human language. *Philos Trans R Soc Lond B Biol Sci* 2011; 366:376-88; PMID:21199842; <http://dx.doi.org/10.1098/rstb.2010.0223>
4. Tomasello M. *Origins of human communication*. Cambridge (Massachusetts): The MIT press, 2008.
5. Stefanatos GA, Baron IS. The ontogenesis of language impairment in autism: a neuropsychological perspective. *Neuropsychol Rev* 2011; 21:252-70; PMID:21842186; <http://dx.doi.org/10.1007/s11065-011-9178-6>
6. Arroyo EJ, Xu T, Poliak S, Watson M, Peles E, Scherer SS. Internodal specializations of myelinated axons in the central nervous system. *Cell Tissue Res* 2001; 305:53-66; PMID:11512672; <http://dx.doi.org/10.1007/s004410100403>
7. O'Dushlaine C, Kenny E, Heron E, Donohoe G, Gill M, Morris D, Corvin A; International Schizophrenia Consortium. Molecular pathways involved in neuronal cell adhesion and membrane scaffolding contribute to schizophrenia and bipolar disorder susceptibility. *Mol Psychiatry* 2011; 16:286-92; PMID:20157312; <http://dx.doi.org/10.1038/mp.2010.7>
8. Vernes SC, Newbury DF, Abrahams BS, Winchester L, Nicod J, Groszer M, Alarcón M, Oliver PL, Davies KE, Geschwind DH, et al. A functional genetic link between distinct developmental language disorders. *N Engl J Med* 2008; 359:2337-45; PMID:18987363; <http://dx.doi.org/10.1056/NEJMoa0802828>
9. Newbury DF, Fisher SE, Monaco AP. Recent advances in the genetics of language impairment. *Genome Med* 2010; 2:6; PMID:20193051; <http://dx.doi.org/10.1186/gm127>
10. Whitehouse AJ, Bishop DV, Ang QW, Pennell CE, Fisher SE. *CNTNAP2* variants affect early language development in the general population. *Genes Brain Behav* 2011; 10:451-6; PMID:21310003; <http://dx.doi.org/10.1111/j.1601-183X.2011.00684.x>
11. Graham SA, Fisher SE. Decoding the genetics of speech and language. *Curr Opin Neurobiol* 2013; 23:43-51; PMID:23228431; <http://dx.doi.org/10.1016/j.conb.2012.11.006>
12. Whalley HC, O'Connell G, Sussmann JE, Peel A, Stanfield AC, Hayiou-Thomas ME, Johnstone EC, Lawrie SM, McIntosh AM, Hall J. Genetic variation in *CNTNAP2* alters brain function during linguistic processing in healthy individuals. *Am J Med Genet B Neuropsychiatr Genet* 2011; 156B:941-8; PMID:21987501; <http://dx.doi.org/10.1002/ajmg.b.31241>
13. Alarcón M, Abrahams BS, Stone JL, Duvall JA, Perederiy JV, Bomar JM, Sebat J, Wigler M, Martin CL, Ledbetter DH, et al. Linkage, association, and gene-expression analyses identify *CNTNAP2* as an autism-susceptibility gene. *Am J Hum Genet* 2008; 82:150-9; PMID:18179893; <http://dx.doi.org/10.1016/j.ajhg.2007.09.005>
14. Arking DE, Cutler DJ, Brune CW, Teslovich TM, West K, Ikeda M, Rea A, Guy M, Lin S, Cook EH, et al. A common genetic variant in the neurexin superfamily member *CNTNAP2* increases familial risk of autism. *Am J Hum Genet* 2008; 82:160-4; PMID:18179894; <http://dx.doi.org/10.1016/j.ajhg.2007.09.015>
15. Bakkaloglu B, O'Roak BJ, Louvi A, Gupta AR, Abelson JF, Morgan TM, Chawarska K, Klin A, Ercan-Sencicek AG, Stillman AA, et al. Molecular cytogenetic analysis and resequencing of contactin associated protein-like 2 in autism spectrum disorders. *Am J Hum Genet* 2008; 82:165-73; PMID:18179895; <http://dx.doi.org/10.1016/j.ajhg.2007.09.017>
16. Peñagarikano O, Geschwind DH. What does *CNTNAP2* reveal about autism spectrum disorder? *Trends Mol Med* 2012; 18:156-63; PMID:22365836; <http://dx.doi.org/10.1016/j.molmed.2012.01.003>
17. Friedman JI, Vrijenhoek T, Markx S, Janssen IM, van der Vliet WA, Faas BH, Knoers NV, Cahn W, Kahn RS, Edelmann L, et al. *CNTNAP2* gene dosage variation is associated with schizophrenia and epilepsy. *Mol Psychiatry* 2008; 13:261-6; PMID:17646849; <http://dx.doi.org/10.1038/sj.mp.4002049>
18. Poot M, Beyer V, Schwaab I, Damatova N, Van't Slot R, Prothero J, Holder SE, Haaf T. Disruption of *CNTNAP2* and additional structural genome changes in a boy with speech delay and autism spectrum disorder. *Neurogenetics* 2010; 11:81-9; PMID:19582487; <http://dx.doi.org/10.1007/s10048-009-0205-1>
19. Rodenas-Cuadrado P, Ho J, Vernes SC. Shining a light on *CNTNAP2*: complex functions to complex disorders. *Eur J Hum Genet* 2013; 22:171-8; PMID:23714751
20. Strauss KA, Puffenberger EG, Huentelman MJ, Gottlieb S, Dobrin SE, Parod JM, Stephan DA, Morton DH. Recessive symptomatic focal epilepsy and mutant contactin-associated protein-like 2. *N Engl J Med* 2006; 354:1370-7; PMID:16571880; <http://dx.doi.org/10.1056/NEJMoa052773>
21. Zweier C. Severe intellectual disability associated with recessive defects in *CNTNAP2* and *NRXN1*. *Mol Syndromol* 2012; 2:181-5; PMID:22670139

22. Lai CS, Fisher SE, Hurst JA, Vargha-Khadem F, Monaco AP. A forkhead-domain gene is mutated in a severe speech and language disorder. *Nature* 2001; 413:519-23; PMID:11586359; <http://dx.doi.org/10.1038/35097076>
23. Fisher SE, Scharff C. FOXP2 as a molecular window into speech and language. *Trends Genet* 2009; 25:166-77; PMID:19304338; <http://dx.doi.org/10.1016/j.tig.2009.03.002>
24. Schneider E, Jensen LR, Farcas R, Kondova I, Bontrop RE, Navarro B, Fuchs E, Kuss AW, Haaf T. A high density of human communication-associated genes in chromosome 7q31-q36: differential expression in human and non-human primate cortices. *Cytogenet Genome Res* 2012; 136:97-106; PMID:22261840; <http://dx.doi.org/10.1159/00035465>
25. Enard W, Przeworski M, Fisher SE, Lai CS, Wiebe V, Kitano T, Monaco AP, Pääbo S. Molecular evolution of FOXP2, a gene involved in speech and language. *Nature* 2002; 418:869-72; PMID:12192408; <http://dx.doi.org/10.1038/nature01025>
26. Ayub Q, Yngvadottir B, Chen Y, Xue Y, Hu M, Vernes SC, Fisher SE, Tyler-Smith C. FOXP2 targets show evidence of positive selection in European populations. *Am J Hum Genet* 2013; 92:696-706; PMID:23602712; <http://dx.doi.org/10.1016/j.ajhg.2013.03.019>
27. Chimpanzee Sequencing and Analysis Consortium. Initial sequence of the chimpanzee genome and comparison with the human genome. *Nature* 2005; 437:69-87; PMID:16136131; <http://dx.doi.org/10.1038/nature04072>
28. Varki A, Altheide TK. Comparing the human and chimpanzee genomes: searching for needles in a haystack. *Genome Res* 2005; 15:1746-58; PMID:16339373; <http://dx.doi.org/10.1101/gr.3737405>
29. Cáceres M, Lachuer J, Zapala MA, Redmond JC, Kudo L, Geschwind DH, Lockhart DJ, Preuss TM, Barlow C. Elevated gene expression levels distinguish human from non-human primate brains. *Proc Natl Acad Sci U S A* 2003; 100:13030-5; PMID:14557539; <http://dx.doi.org/10.1073/pnas.2135499100>
30. Gu J, Gu X. Induced gene expression in human brain after the split from chimpanzee. *Trends Genet* 2003; 19:63-5; PMID:12547510; [http://dx.doi.org/10.1016/S0168-9525\(02\)00040-9](http://dx.doi.org/10.1016/S0168-9525(02)00040-9)
31. Khaitovich P, Enard W, Lachmann M, Pääbo S. Evolution of primate gene expression. *Nat Rev Genet* 2006; 7:693-702; PMID:16921347; <http://dx.doi.org/10.1038/nrg1940>
32. Nowick K, Gernat T, Almaas E, Stubbs L. Differences in human and chimpanzee gene expression patterns define an evolving network of transcription factors in brain. *Proc Natl Acad Sci U S A* 2009; 106:22358-63; PMID:20007773; <http://dx.doi.org/10.1073/pnas.0911376106>
33. Konopka G, Friedrich T, Davis-Turak J, Winden K, Oldham MC, Gao F, Chen L, Wang GZ, Luo R, Preuss TM, et al. Human-specific transcriptional networks in the brain. *Neuron* 2012; 75:601-17; PMID:22920253; <http://dx.doi.org/10.1016/j.neuron.2012.05.034>
34. Xu AG, He L, Li Z, Xu Y, Li M, Fu X, Yan Z, Yuan Y, Menzel C, Li N, et al. Intergenic and repeat transcription in human, chimpanzee and macaque brains measured by RNA-Seq. *PLoS Comput Biol* 2010; 6:e1000843; PMID:20617162; <http://dx.doi.org/10.1371/journal.pcbi.1000843>
35. Liu S, Lin L, Jiang P, Wang D, Xing Y. A comparison of RNA-Seq and high-density exon array for detecting differential gene expression between closely related species. *Nucleic Acids Res* 2011; 39:578-88; PMID:20864445; <http://dx.doi.org/10.1093/nar/gkq817>
36. Jaenisch R, Bird A. Epigenetic regulation of gene expression: how the genome integrates intrinsic and environmental signals. *Nat Genet* 2003; 33(Suppl):245-54; PMID:12610534; <http://dx.doi.org/10.1038/ng1089>
37. Weber M, Hellmann I, Stadler MB, Ramos L, Pääbo S, Rebhan M, Schübeler D. Distribution, silencing potential and evolutionary impact of promoter DNA methylation in the human genome. *Nat Genet* 2007; 39:457-66; PMID:17334365; <http://dx.doi.org/10.1038/ng1990>
38. Molaro A, Hodges E, Fang F, Song Q, McCombie WR, Hannon GJ, Smith AD. Sperm methylation profiles reveal features of epigenetic inheritance and evolution in primates. *Cell* 2011; 146:1029-41; PMID:21925323; <http://dx.doi.org/10.1016/j.cell.2011.08.016>
39. Pai AA, Bell JT, Marioni JC, Pritchard JK, Gilad Y. A genome-wide study of DNA methylation patterns and gene expression levels in multiple human and chimpanzee tissues. *PLoS Genet* 2011; 7:e1001316; PMID:21383968; <http://dx.doi.org/10.1371/journal.pgen.1001316>
40. Wang J, Cao X, Zhang Y, Su B. Genome-wide DNA methylation analyses in the brain reveal four differentially methylated regions between humans and non-human primates. *BMC Evol Biol* 2012; 12:144; PMID:22899776; <http://dx.doi.org/10.1186/1471-2148-12-144>
41. Zeng J, Konopka G, Hunt BG, Preuss TM, Geschwind D, Yi SV. Divergent whole-genome methylation maps of human and chimpanzee brains reveal epigenetic basis of human regulatory evolution. *Am J Hum Genet* 2012; 91:455-65; PMID:22922032; <http://dx.doi.org/10.1016/j.ajhg.2012.07.024>
42. Farcas R, Schneider E, Frauenknecht K, Kondova I, Bontrop R, Bohl J, Navarro B, Metzler M, Zischler H, Zechner U, et al. Differences in DNA methylation patterns and expression of the CCRK gene in human and nonhuman primate cortices. *Mol Biol Evol* 2009; 26:1379-89; PMID:19282513; <http://dx.doi.org/10.1093/molbev/msp046>
43. Schneider E, Mayer S, El Hajj N, Jensen LR, Kuss AW, Zischler H, Kondova I, Bontrop RE, Navarro B, Fuchs E, et al. Methylation and expression analyses of the 7q autism susceptibility locus genes MEST, COPG2, and TSGA14 in human and anthropoid primate cortices. *Cytogenet Genome Res* 2012; 136:278-87; PMID:22456293; <http://dx.doi.org/10.1159/000337298>
44. Anastasiadou C, Malousi A, Maglaveras N, Kouidou S. Human epigenome data reveal increased CpG methylation in alternatively spliced sites and putative exonic splicing enhancers. *DNA Cell Biol* 2011; 30:267-75; PMID:21545276; <http://dx.doi.org/10.1089/dna.2010.1094>
45. Amit M, Donyo M, Hollander D, Goren A, Kim E, Gelfman S, Lev-Maor G, Burstein D, Schwartz S, Postolsky B, et al. Differential GC content between exons and introns establishes distinct strategies of splice-site recognition. *Cell Rep* 2012; 1:543-56; PMID:22832277; <http://dx.doi.org/10.1016/j.celrep.2012.03.013>
46. Gelfman S, Ast G. When epigenetics meets alternative splicing: the roles of DNA methylation and GC architecture. *Epigenomics* 2013; 5:351-3; PMID:23895647; <http://dx.doi.org/10.2217/epi.13.32>
47. Shukla S, Kavak E, Gregory M, Imashimizu M, Shutinoski B, Kashlev M, Oberdoerffer P, Sandberg R, Oberdoerffer S. CTCF-promoted RNA polymerase II pausing links DNA methylation to splicing. *Nature* 2011; 479:74-9; PMID:21964334; <http://dx.doi.org/10.1038/nature10442>
48. Maunakea AK, Nagarajan RP, Bilenky M, Ballinger TJ, D'Souza C, Fouse SD, Johnson BE, Hong C, Nielsen C, Zhao Y, et al. Conserved role of intragenic DNA methylation in regulating alternative promoters. *Nature* 2010; 466:253-7; PMID:20613842; <http://dx.doi.org/10.1038/nature09165>
49. Darling ACE, Mau B, Blattner FR, Perna NT. Mauve: multiple alignment of conserved genomic sequence with rearrangements. *Genome Res* 2004; 14:1394-403; PMID:15231754; <http://dx.doi.org/10.1101/gr.2289704>
50. Darling AE, Mau B, Perna NT. progressiveMauve: multiple genome alignment with gene gain, loss and rearrangement. *PLoS One* 2010; 5:e11147; PMID:20593022; <http://dx.doi.org/10.1371/journal.pone.0011147>
51. Fedrigo O, Warner LR, Pfefferle AD, Babbitt CC, Cruz-Gordillo P, Wray GA. A pipeline to determine RT-QPCR control genes for evolutionary studies: application to primate gene expression across multiple tissues. *PLoS One* 2010; 5:e12545; PMID:20824057; <http://dx.doi.org/10.1371/journal.pone.0012545>
52. Vandesompele J, De Preter K, Pattyn F, Poppe B, Van Roy N, De Paeppe A, Speleman F. Accurate normalization of real-time quantitative RT-PCR data by geometric averaging of multiple internal control genes. *Genome Biol* 2002; 3:H0034; PMID:12184808; <http://dx.doi.org/10.1186/gb-2002-3-7-research0034>
53. Livak KJ, Schmittgen TD. Analysis of relative gene expression data using real-time quantitative PCR and the 2(-Delta Delta C(T)) Method. *Methods* 2001; 25:402-8; PMID:11846609; <http://dx.doi.org/10.1006/meth.2001.2001.1262>
54. Ruf N, Bähring S, Galetzka D, Pliushch G, Luft FC, Nürnberg P, Haaf T, Kelsey G, Zechner U. Sequence-based bioinformatic prediction and QUASEP identify genomic imprinting of the KCNK9 potassium channel gene in mouse and human. *Hum Mol Genet* 2007; 16:2591-9; PMID:17704508; <http://dx.doi.org/10.1093/hmg/ddm216>
55. Jones S, Martin R, Pilbeam D. The Cambridge encyclopedia of human evolution. Cambridge (UK): Cambridge University Press, 2000.
56. Ruff CB, Trinkaus E, Holliday TW. Body mass and encephalization in Pleistocene Homo. *Nature* 1997; 387:173-6; PMID:9144286; <http://dx.doi.org/10.1038/387173a0>
57. Holliday R, Grigg GW. DNA methylation and mutation. *Mutat Res* 1993; 285:61-7; PMID:7678134; [http://dx.doi.org/10.1016/0027-5107\(93\)90052-H](http://dx.doi.org/10.1016/0027-5107(93)90052-H)
58. Olson MV, Varki A. Sequencing the chimpanzee genome: insights into human evolution and disease. *Nat Rev Genet* 2003; 4:20-8; PMID:12509750; <http://dx.doi.org/10.1038/nrg981>
59. Gladkevich A, Kauffman HF, Korf J. Lymphocytes as a neural probe: potential for studying psychiatric disorders. *Prog Neuropsychopharmacol Biol Psychiatry* 2004; 28:559-76; PMID:15093964; <http://dx.doi.org/10.1016/j.pnpbp.2004.01.009>
60. Davies MN, Volta M, Pidsley R, Lunnon K, Dixit A, Lovestone S, Coarfa C, Harris RA, Milosavljevic A, Troakes C, et al. Functional annotation of the human brain methylome identifies tissue-specific epigenetic variation across brain and blood. *Genome Biol* 2012; 13:R43; PMID:22703893; <http://dx.doi.org/10.1186/gb-2012-13-6-r43>
61. Hill H, Ott F, Herbert C, Weisbrod M. Response execution in lexical decision tasks obscures sex-specific lateralization effects in language processing: evidence from event-related potential measures during word reading. *Cereb Cortex* 2006; 16:978-89; PMID:16177269; <http://dx.doi.org/10.1093/cercor/bhj040>
62. Crow TJ. The 'big bang' theory of the origin of psychosis and the faculty of language. *Schizophr Res* 2008; 102:31-52; PMID:18502103; <http://dx.doi.org/10.1016/j.schres.2008.03.010>

63. Feuk L, Kalervo A, Lipsanen-Nyman M, Skaug J, Nakabayashi K, Finucane B, Hartung D, Innes M, Kerem B, Nowaczyk MJ, et al. Absence of a paternally inherited FOXP2 gene in developmental verbal dyspraxia. *Am J Hum Genet* 2006; 79:965-72; PMID:17033973; <http://dx.doi.org/10.1086/508902>
64. Kelsey G. Genomic imprinting--roles and regulation in development. *Endocr Dev* 2007; 12:99-112; PMID:17923773
65. Ideraabdullah FY, Vigneau S, Bartolomei MS. Genomic imprinting mechanisms in mammals. *Mutat Res* 2008; 647:77-85; PMID:18778719; <http://dx.doi.org/10.1016/j.mrfmmm.2008.08.008>
66. Reik W, Constância M, Fowden A, Anderson N, Dean W, Ferguson-Smith A, Tycko B, Sibley C. Regulation of supply and demand for maternal nutrients in mammals by imprinted genes. *J Physiol* 2003; 547:35-44; PMID:12562908; <http://dx.doi.org/10.1113/jphysiol.2002.033274>
67. Gregg C, Zhang J, Weissbourd B, Luo S, Schroth GP, Haig D, Dulac C. High-resolution analysis of parent-of-origin allelic expression in the mouse brain. *Science* 2010; 329:643-8; PMID:20616232; <http://dx.doi.org/10.1126/science.1190830>
68. Ubeda F, Gardner A. A model for genomic imprinting in the social brain: juveniles. *Evolution* 2010; 64:2587-600; PMID:20394663; <http://dx.doi.org/10.1111/j.1558-5646.2010.01015.x>
69. Ubeda F, Gardner A. A model for genomic imprinting in the social brain: adults. *Evolution* 2011; 65:462-75; PMID:20812976; <http://dx.doi.org/10.1111/j.1558-5646.2010.01115.x>
70. Brown WM. The parental antagonism theory of language evolution: preliminary evidence for the proposal. *Hum Biol* 2011; 83:213-45; PMID:21615287; <http://dx.doi.org/10.3378/027.083.0205>
71. Moore T, Haig D. Genomic imprinting in mammalian development: a parental tug-of-war. *Trends Genet* 1991; 7:45-9; PMID:2035190
72. Thomas AC, Frost JM, Ishida M, Vargha-Khadem F, Moore GE, Stanier P. The speech gene FOXP2 is not imprinted. *J Med Genet* 2012; 49:669-70; PMID:23033221; <http://dx.doi.org/10.1136/jmedgenet-2012-101242>
73. Semendeferi K, Armstrong E, Schleicher A, Zilles K, Van Hoesen GW. Prefrontal cortex in humans and apes: a comparative study of area 10. *Am J Phys Anthropol* 2001; 114:224-41; PMID:11241188; [http://dx.doi.org/10.1002/1096-8644\(200103\)114:3<224::AID-AJPA1022>3.0.CO;2-I](http://dx.doi.org/10.1002/1096-8644(200103)114:3<224::AID-AJPA1022>3.0.CO;2-I)
74. Enard W, Pääbo S. Comparative primate genomics. *Annu Rev Genomics Hum Genet* 2004; 5:351-78; PMID:15485353; <http://dx.doi.org/10.1146/annurev.genom.5.061903.180040>
75. Benton MJ, Donoghue PCJ. Paleontological evidence to date the tree of life. *Mol Biol Evol* 2007; 24:26-53; PMID:17047029; <http://dx.doi.org/10.1093/molbev/msl150>
76. Knussmann R. Anthropologie. Handbuch der vergleichenden Biologie des Menschen. Bd 1/1. Stuttgart: G. Fischer Verlag, 1988.
77. Goodall J. Population dynamics during a 15 year period in one community of free-living chimpanzees in the Gombe national park, Tanzania. *Z Tierpsychol* 1983; 61:1-60; <http://dx.doi.org/10.1111/j.1439-0310.1983.tb01324.x>
78. Chavez L, Jozefczuk J, Grimm C, Dietrich J, Timmermann B, Lehrach H, Herwig R, Adjaye J. Computational analysis of genome-wide DNA methylation during the differentiation of human embryonic stem cells along the endodermal lineage. *Genome Res* 2010; 20:1441-50; PMID:20802089; <http://dx.doi.org/10.1101/gr.110114.110>